The influence of Mount Sinabung eruption on the geothermal in Tinggi Raja Simalungun

Togi Tampubolon [a,*], Jeddah Yanti [b], Rita Juliani [a], Juniar Hutahaean [a]

[a] *Department of Physics, Faculty of Mathematics and Natural Science, State University of Medan, 20221, Medan, North Sumatra, Indonesia*
[b] *Department of Geography, Faculty of Mathematics and Natural Science, State University of Makassar, 90222, South Sulawesi, Indonesia*

ARTICLE INFO

ABSTRACT

Mount Sinabung is a Pleistocene-to-Holocene stratovolcano, and its 2010 eruption was the first active activity after having been dormant for a long time. Enhanced pressure, intensity, and thermal energy of Sinabung activities hit several geothermal resources and triggered Tinggi Raja geofluid in Simalungun. This study aims to identify Sinabung eruption influences the appearance and point-transfer movement of geothermal features in Tinggi Raja. This research method builds a field model analysis (FMA) by integrating the quantitative and qualitative approaches focused on historic earthquakes activities (HEA) from the Center of Volcanology and Geological Hazard Mitigation (CVGHM), time-series satellite observation of land surface change, and land surface temperature, the residual anomaly of the geothermal reservoir, high altitudes and chemical-drop in pH, and point-transfer movement. HEA shows fluctuating activities in eruption level or Volcanic Eruption Index (VEI) scale. FMA offers fewer residual anomalies from Southwest to Northeast in 100 m–600 m coverage 5 km^2 underground than pre-hypothesis indicates the anomaly zone associated with the fracture zone; however, the lithology of the geothermal system is categorized as limestone rock and has no active faults. It indicates a low magnetic field anomaly in geothermal resources that does not correlate volcanic manifestation to geothermal trigger. Distance, type, and felt volcanic earthquake and eruption are less direct impact between the eruption of Mount Sinabung and the displacement of springs at Tinggi Raja.

1. Introduction

Mount Sinabung is an active stratovolcano with a 2460 m located in Karo district North Sumatera over Sumatera faults and supervolcano Toba (Kabupaten Karo, 2021). No past signs of exploding, but it became involved in early 2000; the first eruptions from Mt Sinabung produced magmatic gases in 2010 (BNPB, 2013; BNPB, 2016). Those eruptions of Mount Sinabung began with a shallow earthquake to mainshock in September 2010 and released high gas pressure with an volcanic eruption column height of approximately 500 m, leaning on the southeast (Center for Volcanology and Geological Hazard Mitigation, 2020). Twenty-eight cases of Mount Sinabung dramatically erupted in a vertical plume consisting of a super-heated ash cloud and tephra suspended in gases with high-speed movements to the slopes. Around 3000 residents of Mount Sinabung evacuated. Significant eruptions continue today.

Based on geology, North Sumatera has complex structural and physical characteristics of rocks in many collisions of the Eastern Eurasian and Western Australian destructive plate boundary. The conditions that cause a fault, fracture, and folding path over North Sumatera through an Alas – Karo segmentation in 390 km result in volcanic eruptions, landslides, and geothermal triggering (Kabupaten Karo, 2021). High fault, fracture, and folding path pressure cause geothermal manifestation under the Earth's surface. The geothermal area can manifest in jetting hydrothermal fluids, an area of high heat flow dissolved underground until the gas pressure exsolve as the hot springs approach the Earth's surface (Primulyana et al., 2019). The frequency of hydrothermal explosions (steam and hot spring) has a heat flow of 50–75 °C (Yan et al., 2022).

Many research observed that the Simalungun regency has potentially hydrothermal resources in Silau Kahean district, Tinggi Raja, and Dolok Morawa since 2006 (Sundhoro et al., 2006). This area has a temperature of around 180 °C, categorized as sensible enthalpy with potential energy resources around 49 to 50 MWe. The hydrothermal vent in Tinggi Raja moves approximately 40–80 m from the last hotspot (Kab Simalungun, 2021). Previous research monitored hydrothermal in Yellow-stone National Park by utilizing thermal infrared from remote sensing technology

---

* Corresponding author.
  E-mail address: topartam@gmail.com (T. Tampubolon).

Fig. 1. Mount Sinabung on the big eruption in 2015.

(Neale et al., 2016). The previous analysis illustrated that GIS and aeromagnetic data map changes the structure and characteristics of hydrothermal matter in Wadi Allaqi, Egypt (Mohamed El-Desoky et al., 2021). Eskandari et al., 2015, utilized remote sensing technology using Landsat image to implicate volcanological dynamics in Damavand, Iran (Eskandari et al., 2015). Marwan et al., 2021, conducted indirect connecting faults and hydrothermal systems in Seulawah volcano from magnetotellurics structure (Marwan et al., 2021).

Based on existing studies, conceptual models have proved the emergence of hot springs adjacent to normal fault scarps to establish fluid circulation patterns and build possible thermal anomalies. Involving magmatic activity is responsible for transferring in the crust and impacting liquid precipitate as evidence of hydrothermal circulation. A practical time-series imaging and monitoring structure of the Tinggi Raja hydrothermal features and Sinabung activities to enhance the identification, characterization, and regulation of eruptive dynamism depends on hydrothermal circulation. Previous studies of Sinabung activities are essentially based on analytical solutions of a single method, but none of them could provide field model analysis consistently.

Therefore, the multiscale approach depends on (1) Integration of historical activities from numerous historical eruptions has occurred from 2010 until 2021, the Center of Volcanology and Geological Hazard Mitigation (CVGHM); (2) observation of the time-series satellite land surface change and land surface temperature with GIS and remote sensing techniques; (3) consideration of the geomagnetic anomaly of the geothermal reservoir, high altitudes and chemical-drop in pH, and point-transfer movement can create impending path eruption into field model and prepare nearby populations and endanger residents' safety for potentially volcanic hazard (Sullivan and Sagala, 2020). The research aims to identify the relationship between Mount Sinabung eruption with Hydrothermal resources through geophysics field study and remote sensing techniques.

2. Study area

Mount Sinabung is located in the Karo Plateau, Karo regency, North Sumatra, Sumatra island at 3°10' North Latitude and 98°23.5' East
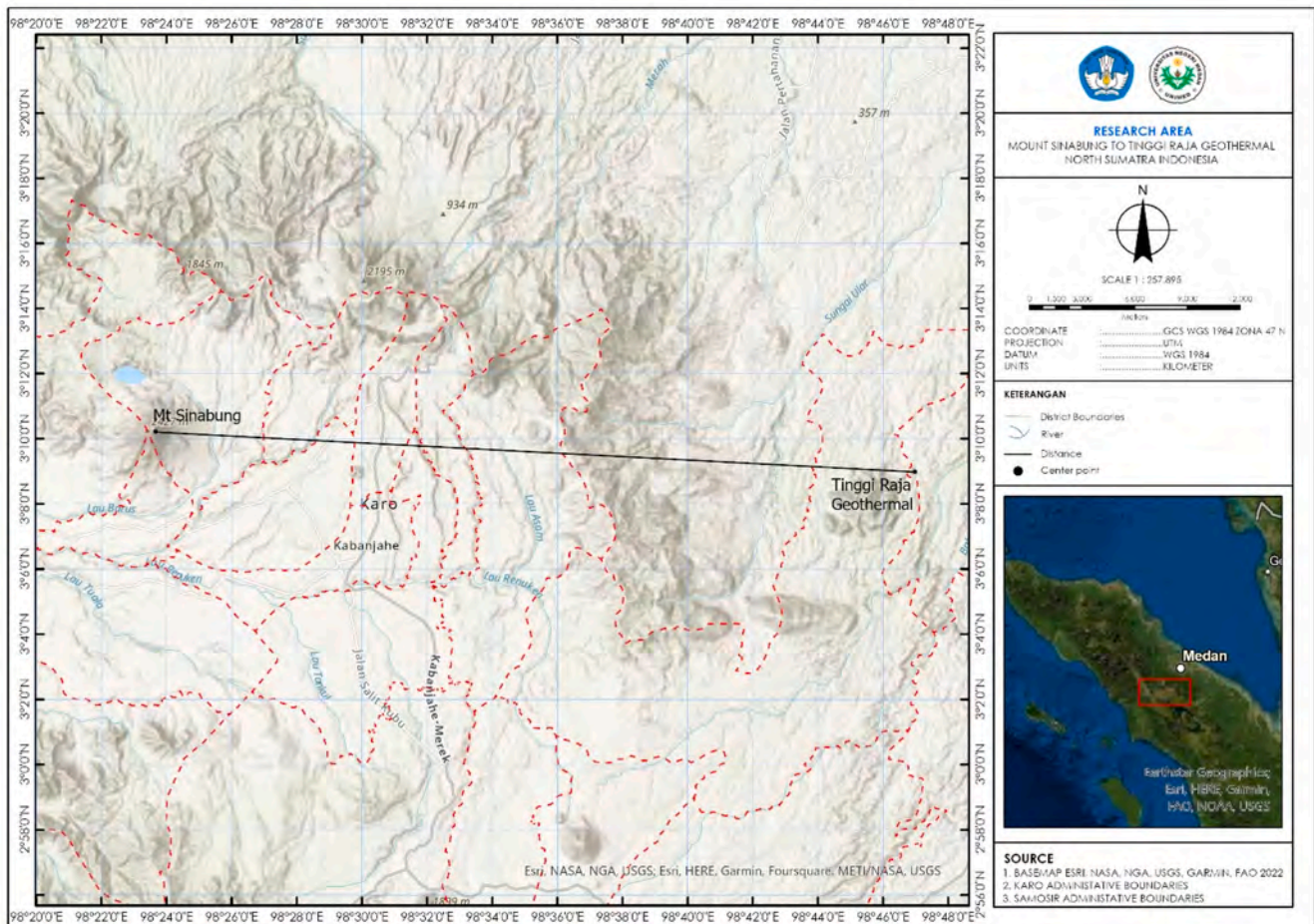

Fig. 2. Research area with a combined geographical location of Mount Sinabung and Tinggi Raja geothermal area, Simalungun District.
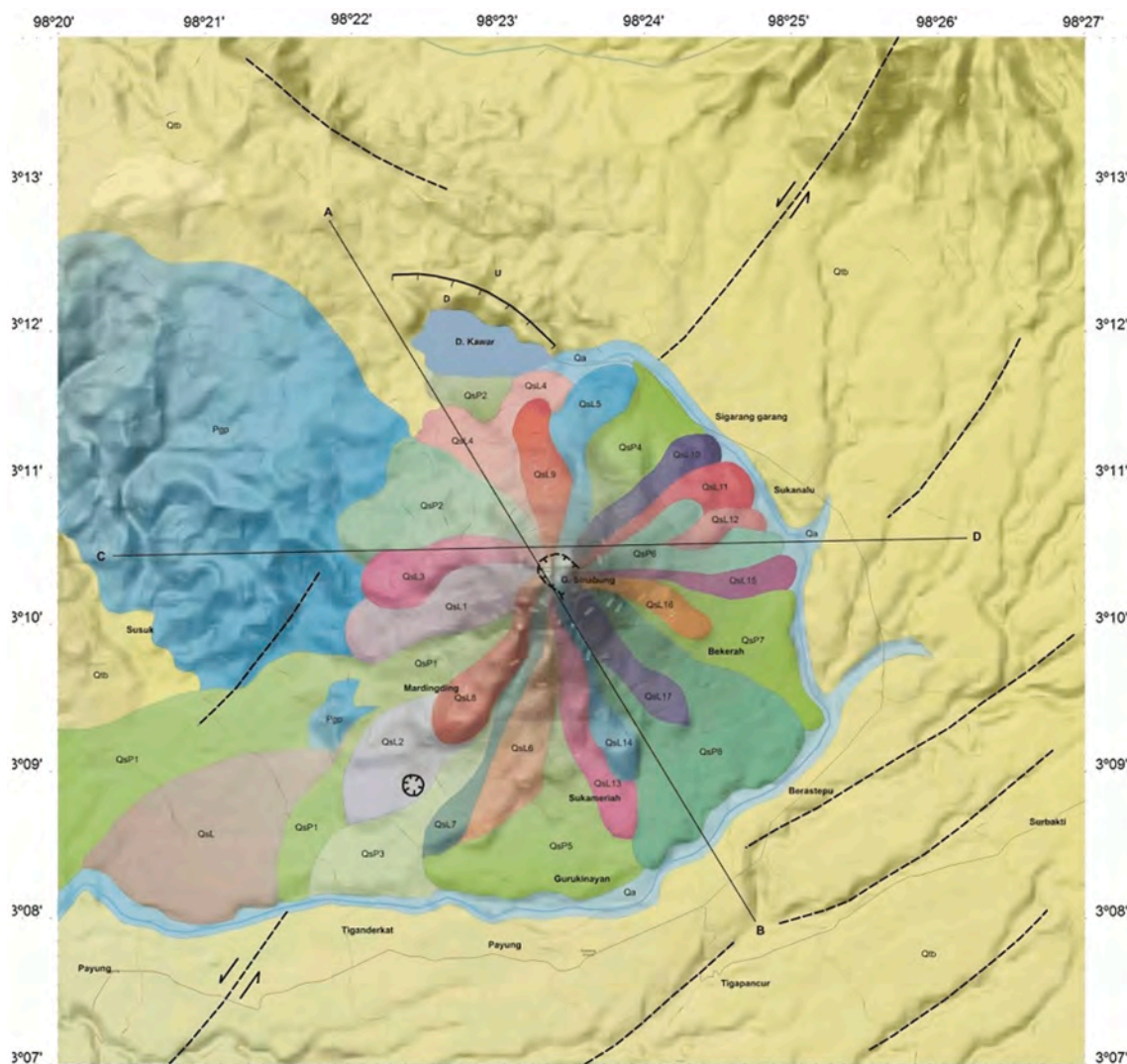
Fig. 3. Geological map of Mount Sinabung, North Sumatra Province (Indrastuti et al., 2019).

Longitude, with an altitude of 2460 m above mean sea level. One of the most significant volcanic eruptions of Mount Sinabung occurred in 2015 (Fig. 1). Sumatra Island also has the potential of geothermal resources of 13,470 MW and is the most considerable potential compared to other islands (Center for Volcanology and Geological Hazard Mitigation, 2020). A hot spring was found in Simalungun Regency, namely the Kawah Putih, Tinggi Raja, located in Silau Kahean Subdistrict; Dolok Marawa Village. Kawah Putih is part of the cross position in the Western Pacific Trench region, which is geographically located between 02°36'-03°18' North Latitude and 98°32' - 99°35' East Longitude (Fig. 2) (Kab Simalungun, 2021). The average distance between Mount Sinabung and Tinggi Raja is ±44 km (27,34 miles). Volcanic landform can provide level geological information of Sinabung that the Central Volcanology Agency created in Bandung can be seen in Fig. 3 (Indrastuti et al., 2019).

3. Methodology

Field model analysis (FMA) build by integrating quantitative and qualitative essential aspects. The qualitative assessment is performed considering the investigation of the geology and eruptive history of Mount Sinabung. It appears as a critical step for observation of volcanic landform, and historic earthquakes activities (HEA) belongs to the information on series (hours, dates, months, years), strength, and

direction of earthquakes from the Center of Volcanology and Geological Hazard Mitigation (CVGHM) from 2015 until 2021 (Gunawan et al., 2019). Tracking field surveys in Tinggi Raja, collecting GPS points, taking physical evidence in active and inactive spring resources, and interviewing resident communities around geothermal areas as quantitative assessments (Andreastuti et al., 2019).

Approaches to landscape changes and land surface temperature properties from the first eruption will continue based on analysis of Landsat images provider of Mount Sinabung and Tinggi Raja, supplemented with measures and field observation made at high altitudes and chemical-drop in pH and spring point-transfer displacement in Tinggi Raja. GIS (geographic information system) and remote sensing methods characterize the landscape detachment and land surface temperature. Attribute data and spatial data of Landsat satellite extracted data analysis using ArcGIS Pro and ENVI 4.7 from 2015 until 2021.

Land surface change is calculated considering time-series NDVI (normalized difference vegetation) index in equation (1) and LST (land surface temperature) index in equation (1). NIR is light reflected in the near-infrared spectrum, RED is light reflected in the red spectrum, K_1 and K_2 mean spectrum-specific thermal conversion constant from metadata, and L_λ implies top of atmospheric (TOA) spectral radiance from thermal spectrum.

Table 1
Activities record of Mount Sinabung.

No.	Time	Information
1.	27 August 2010	The term volcanic ash and smoke.
2.	29 August 2010 (00.15 a.m.)	Produced lava.
3.	03 September 2010	There were two eruptions. 1. at 4:45 a.m. (spitting out 3 km of volcanic dust). 2. at 18.00 (co-occurs with a volcanic earthquake which can be felt up to 25 km around the mountain).
4.	07 September 2010	There was a big eruption; the eruption sound was heard up to 8 km, and volcanic dust spread up to 5,000 m in the air.
5.	15 September 2013	It happens in the early hours of the morning and evening.
6.	17 September 2013	Two eruptions occurred day and night, releasing hot clouds and volcanic ash.
7.	03 November 2013 (03.00 a.m.)	Eruptions accompanied a glide of hot clouds up to 1.5 km.
8.	20 November 2013	There have been six eruptions since early morning.
9.	23 November 2013	Eruption (eruption) occurred four times Hot-clouds in the mountain area.
10.	24 November 2013	There was an eruption five times, forming an 8000m high ash pool on peak of mountain.
11.	24 November 2013 (10.00 a.m.)	The status of Mount Sinabung is raised to the highest level, level four (beware).
12.	03 January 2014	Incandescent lava and hot cloud bursts occur.
13.	04 January 2014	There was a series of earthquakes, eruptions and glides of hot clouds.
14.	26 June 2015	More than 28 pyroclastic flows - surges of hot ash and gas that rush down the side of the mountain at high speed, fearing a ***major eruption.***
15.	21 May 2016 (04.48 p.m.)	An eruption caused a hot cloud.
16.	22 Mei 2016	There were four eruptions.
17.	19 February 2018 (08.53 a.m.)	Eruptions occur and emit ash and hot clouds. Level four (Beware).
18.	06 April 2018 (05.30 p.m.)	An earthquake occurs by spewing hot.
19.	07 May 2019 (07.28 a.m.)	The height of the eruption ash column from Mount Sinabung was observed to be approximately 2,000 m above the peak or 4,460 m above sea level.
20.	02 November 2020 (11.58 p.m.)	The height of the ash column was observed to be ±1500 m above the peak (±3960 m above sea level). The ash column is gray with thick intensity towards the east.
21.	03 January 2021	This volcano erupted with an ash pool as high as 500 m into the sky.
22.	19 July 2021 (07.01 p.m.)	The height of the ash column was observed to be ±300 m above the peak (±2760 m above sea level). The ash column is gray with thick intensity to the east and southeast. This eruption was recorded on a seismograph with a maximum amplitude of 47 mm and a duration of 605 s.

$$NDVI = \frac{NIR - RED}{NIR + RED} \qquad (1)$$

$$LST = \left(\frac{K_2}{ln\left(\frac{K_1}{L_\lambda}+1\right)}\right) \qquad (2)$$

Another factor is measuring and modeling residual magnetic anomaly calculated based on parameters. The geomagnetic method is based on measurements of geomagnetic anomalies caused by differences in the contrast of the susceptibility or magnetic permeability of the trap body of the surrounding area (Sharma, 2012; Li and Fu, 2019). It includes magnetized position, inclination, declination of the object to show rocks profile, faults finding, and the possibility of finding magma forming rocks in-depth level of 12–20 km at of hydrothermal phase in Tinggi Raja (Hotta et al., 2019). Within all categories defined above, FMA is a combined qualitative and quantitative assessment that performs a numerical model obtained using interconnected-principle calculation.

4. Results

A consistent number of Sinabung records on significant eruptions from 2010 until 2021 is illustrated by historic earthquake activities (HEA) information on series (hours, dates, months, years), strength, and direction of earthquakes. The last eruption occurred on July 2021 and continues today. Mount Sinabung's activities can be seen in Table 1 below. HEA shows the most extended period and immense voluminous known outpouring of lava from Sinabung Volcano in more than one decade. Lava dome, flow-forming eruption, volcanic ash, and rock fragments have profoundly changed the landscape, disrupted the crop field, and repeatedly challenged residents with lava inundation (Carr et al., 2019). HEA built a better understanding of Sinabung's volcanology in the past and made things the way to help mitigate processes today. HEA can be referenced for the researcher to understand past volcanic events before multi-series satellite information is provided.

Volcano eruption measurements (bursts of smoke/ash or plume) are essential as one measure to determine the eruption rate (Volcanic Eruption Index or VEI scale) (Karolina et al., 2015; Nakada et al., 2019). The VEI scale is divided into eight levels: level 0 - level 7. The higher the eruption level or the VEI scale, the higher the smoke/ash burst (plume) formed and the volume of the eruption material. Mount Sinabung's activity indicates a curious eruption level (Volcanic Eruption Index or VEI scale). It can be seen in Table 2.

Long-term impact of eruption in volcanological records affects how the landscape around the study area is formed—adverse effects to significant shape changes calculated by the NDVI index are shown in Fig. 4. The graph illustrates how the NDVI index scale was reported to have time-series changes in the study area from 2015 to 2021. Overall, the number of NDVI values decreased over the period given. The highest distribution of NDVI values can be seen in past-event. Reducing the path of NDVI distribution indicates that the landscape is formed into non-vegetated features. Match-making analysis shows landscape evolving with Sinabung volcano logical record at the same-range timeline. When volcanoes erupt, hot lava, and hot clouds are spewed from inside amid weather conditions. With the strength and direction of a lava flow, rock is formed, which can change the shape and temperature of the study area (Carr et al., 2019). Overall, the number of NDVI values increased over the period given. The highest distribution of NDVI values can be seen in past-event. Increasing the path of LST distribution indicates that the temperature rose when non-vegetated features. Match-making analysis shows temperature changes with Sinabung volcano logical record at the same-range timeline (Pallister et al., 2019; Reda et al., 2022).

Point-view of active hydrothermal spring in 47N 0476673 UTM 0348563 to 47N 0476300 UTM 0347903 and lost or inactive hydrothermal spring in 47N 0476321 can be seen in Fig. 5. Interviewing results from resident communities around hydrothermal areas assume lost-found or point-transfer movement of geothermal features in

Table 2
Eruption Levels (Volcanic Eruption Index or VEI scale) of Mount Sinabung of Mount Sinabung.

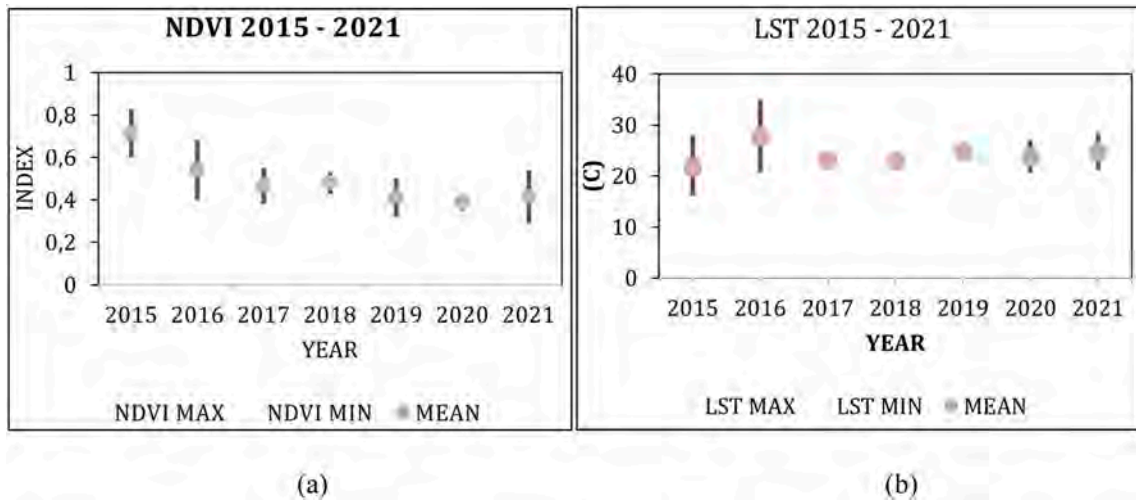| Start Date	Stop Date	Eruption Certainty	VEI	Evidence	Activity Area or Unit
15 September 2013	22 June 2018	Confirmed	4	Historical Observations	
27 August 2010	18 September 2010	Confirmed	2	Historical Observations	
[1881]	[Unknown]	*Uncertain*			
0810 ± 70 years	Unknown	Confirmed		Radiocarbon (corrected)	SE flank

Fig. 4. (a) The distribution of NDVI values (b) LST values from 2015 to 2021 in study area.
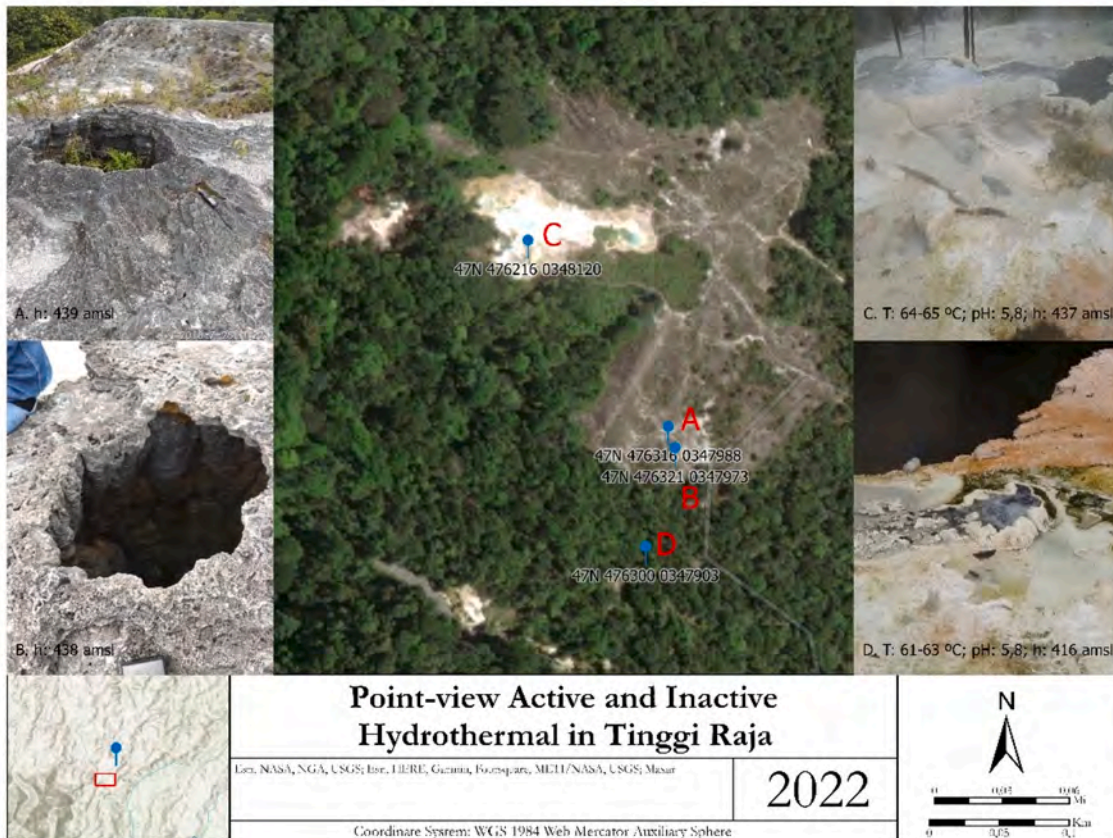

Fig. 5. Point-view (a), (b) inactive hydrothermal spring and (c), (d) active hydrothermal spring in Tinggi Raja.

Tinggi Raja in range-time of Sinabung eruption (Kab Simalungun, 2021; Sullivan and Sagala, 2020).

As a field survey, the geomagnetic and gravity anomaly result in Tinggi Raja shows a high anomaly zone around the A to A′ line. It is associated with high-density rocks such as lava or intrusive rocks. A to A's quantitative model interpretation showed the presence of sediment and calcite rocks, with a susceptibility value of −0.002; 0,006; 0.002; and 0.015 can be seen in Fig. 6 (Awaliyatun and Hutahaean, 2015). The variation of magnetic field strength in each point with the intensity value. From the qualitative interpretation results, the magnetic anomaly value was from −11.8533 nT to 34.6033 nT. The 3D modeling results show low resistivity values at a depth of about 100 m–500 m with a longitudinal pattern from the southwest to the northeast (Nugraha et al., 2019). Lowel-type prisoners' value in the middle of the surrounding manifestations is interpreted as a response to alteration rocks that are thought to act as hoods (Indrastuti et al., 2019).

Geothermal exploration can be determined by identifying the rock resistivity value using several methods such as electromagnetic, gravitational, seismic, geomagnetic, and geoelectric. Of these several methods, geomagnetic and geoelectric methods have many advantages. The geomagnetic method is carried out based on measurements of geomagnetic anomalies caused by differences in the contrast of the
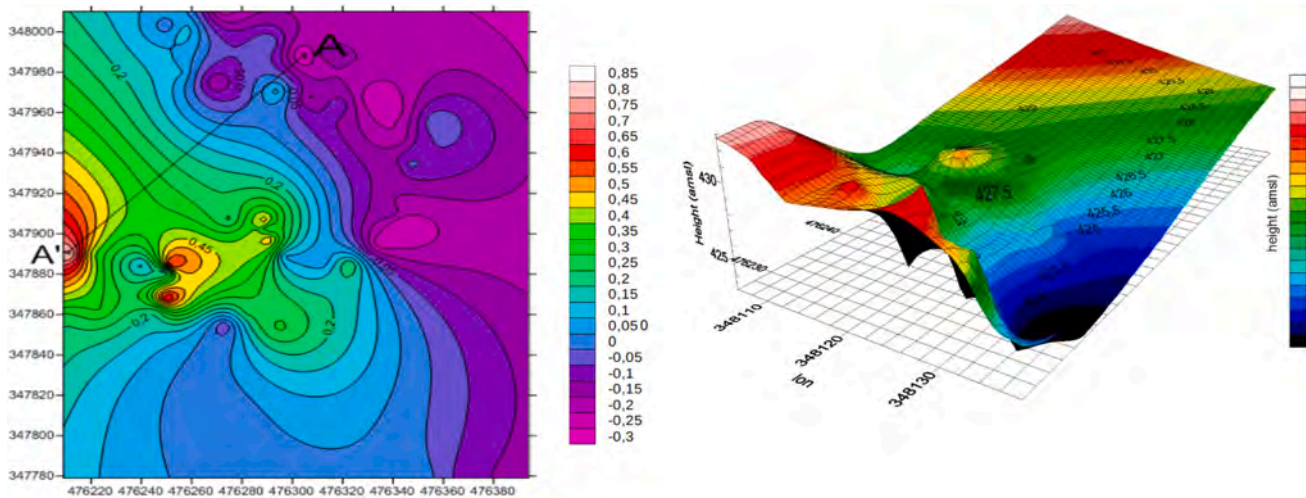
Fig. 6. The distribution of geomagnetic and gravity anomaly in Tinggi Raja.

Fig. 7. Inactive faults found in Tinggi Raja and geological map of rocks and faults distribution.

susceptibility or magnetic permeability of the trap body of the surrounding area (Li and Fu, 2019). The difference in relative permeability is caused by differences in the distribution of ferromagnetic minerals, paramagnetic and diamagnetic. This geomagnetic method is sensitive to abrupt changes, generally used to study intrusive bodies, bedrock, and hydrothermal rich in ferromagnetic minerals and geological structures. For example, Patuha geothermal area shows the presence of magnetic anomalies in tuffs, terfa lapilli, andesite pyroclastic, andesite, and andesite breccia are varying susceptibility values, k, from -0.03 to 0.25 (in units cgs) (Ashat et al., 2019). Permeable rock layers cause magnetic anomalies around manifestations. This layer is estimated as a reservoir predicted as younger andesite and a source of geothermal energy. Oktaviani and Kadri's research (2018) in the Sibual-bual mountain area shows that the geothermal area has varying resistivity, around 1.27–13.8 μm. Geothermal layers are at a depth of 1.25–6.00 m. A layer with a resistivity value of <14 Ωm, this layer is interpreted as a silt soil layer. From a depth of 1.25–12.4 m, the soil or rock is silt soil, clay soil, and soft wet clay soil (Octavani and Kadri, 2019). From previous research, geomagnetic and geoelectric methods were effective methods to find out the point of the prospect of geothermal energy (Ekinci et al., 2014). One geothermal prospect area in the Simalungun district locates at 02°36-15 ″-03°18-06″ LU and 98°32'06" - 99°34'28″ BT.

More significant residual anomalies indicate the presence of resistive rocks in the form of limestone and intrusive rocks. Among the values of high types of detainees and the value of low-type detainees (the central part around the manifestation), a moderate variety of residual anomalies values is estimated in response to the reservoir zone. The peak of the reservoir zone is at a depth of about 500 m. Based on the integrated gravity compilation, the prospect of geothermal heat is estimated to be in the site of low residual gravity force anomalies associated with the fracture zone and the zone of moderate type residual anomalies values related to the active location. The prospect area is the nearest manifestation and extends to the northwest and southeast with about 5 km^2. All information can be seen in Fig. 6. However, an on-field survey found a non-active fracture with a low anomaly zone around the Tinggi Raja hot spring, which can be seen in Fig. 7.

Fig. 7 explained that the area between Mount Sinabung - Tinggi Raja was in the West to East direction, with several rocks and faults. Four types of rocks contained Qvsn, so-called andesite lava to dacite, Qvbj, so-called Binjai Unit: Breccia andesite to the dacite, QTvk, so-called Takur-takur Unit: Andesite, Dacite, and Piroclastics, and Qvt, so-called Toba Tufa: Riodacite tufa, partially released (Bhakti, 2011).

The fault type between Mount Sinabung and Tinggi Raja is a non-active (local) fault because of the active fault position found on Sumatra Island, far from the Mount Sinabung and Tinggi Raja areas. The inactive faults found between Mount Sinabung and Tinggi Raja are
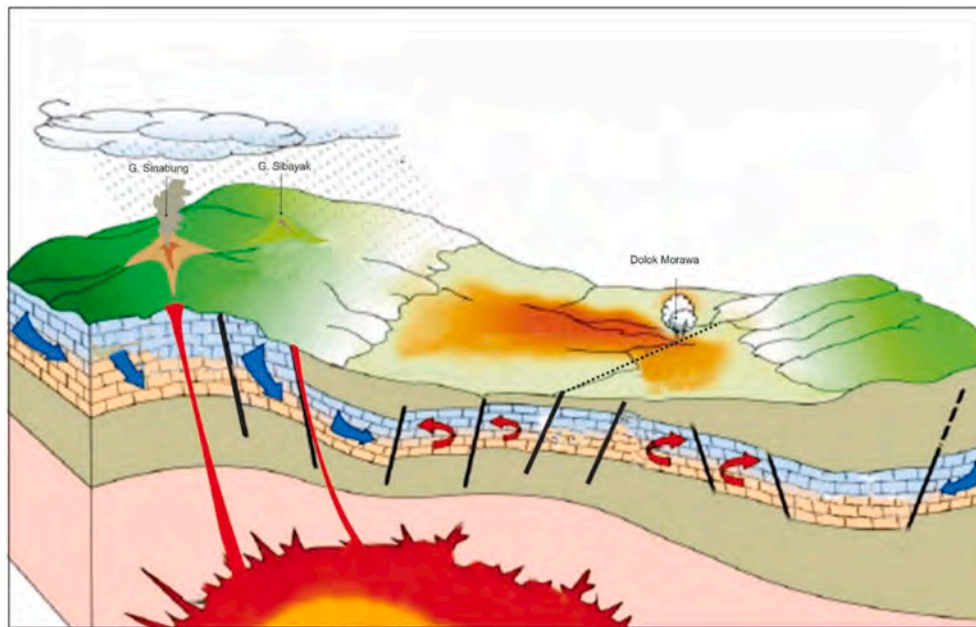
Fig. 8. FMA shows slice of area between Mount Sinabung and Tinggi Raja's geothermal, Dolok Morawa, Simalungun District.

between Mount Sinabung and Mount Sibayak, faults through around Kutagugung to Lingga; Tongkoh to Tanjung Barus, pass L.Dadape, pass Ujung Meriah towards Mount Sinembah, to Tinggi Raja (Nukman and Hochstein, 2019).

In Fig. 8, Field modeling analysis is referred to virtual-model by integrating the quantitative and qualitative approaches focused on historic earthquakes activities (HEA) from the Center of Volcanology and Geological Hazard Mitigation (CVGHM), time-series satellite observation of land surface change, and land surface temperature, the residual anomaly of the geothermal reservoir, high altitudes and chemical-drop in pH, and point-transfer movement. FMA shows surface and subsurface information; surface information illustrates landscape and land surface temperature changes during the period given, and subsurface shows heat flow under the point-view of an active geothermal spring in the study area. FMA offers fewer residual anomalies from Southwest to Northeast in 100 m–600 m coverage 5 km^2 underground than prehypothesis indicates the anomaly zone associated with the fracture zone; however, the lithology of the geothermal system is categorized as limestone rock and has no active faults. It indicates a low magnetic field anomaly in geothermal resources that does not correlate volcanic manifestation to geothermal trigger. Distance, type, and felt volcanic earthquake and eruption are less direct impact between Mount Sinabung eruption and the displacement of springs at Tinggi Raja (Kriswati et al., 2019).

Furthermore, subsurface information from FMA has limited information because geomagnetic dipatching in wide-area. So, FMA indicates the obstruction of the surface in a hot spring due to heating the water fluid high enough continuously, causing clumping of hot water (travertine) in the outlet of the hot water in the fault field. As a result, the travertine heap will cover the flow of hot water on the surface so that hot water with higher pressure searches for new output channels as if creating new hot springs or the transfer of hot springs on the surface (Mccausland et al., 2019).

The further finding indicates that the Tinggi Raja geothermal in Simalungun has a prospect of geothermal energy potential. Simalungun, North Sumatra, is located in the western Pacific trough area, so there are heat energy sources of white and blue craters, one of the areas that have the potential for geothermal precisely in the village of Tinggi Raja.

5. Discussion

Because of its distance, type of felt volcanic earthquake, and evolution of complex shield eruption, Field Model Analysis are worthily related to the possibility that Mount Sinabung might hold onto the geothermal reservoir in Tinggi Raja (Kriswati et al., 2019). Fig. 8 summarizes our observations in a conceptual model of volcanic manifestation to geothermal trigger. The physical properties and state of geothermal resources in Tinggi Raja have visible hydrothermal features on an irregular travertine deposit surrounding andesite, dacite, and pyroclastic rocks. Because of its distance, type of felt volcanic earthquake, and evolution of complex shield eruption, Field Model Analysis are worthily related to the possibility that Mount Sinabung might hold onto the geothermal reservoir in Tinggi Raja. Fig. 8 summarizes our observations in a conceptual model of volcanic manifestation to geothermal trigger. FMA is concerned with the physical properties and state of geothermal resources in Tinggi Raja that have visible hydrothermal features on an irregular travertine deposit surrounding andesite, dacite, and pyroclastic rocks. This result is consistent with Bhakti (2011), who showed that extrusive rock in the Tinggi Raja Karo district tends to be identical to young-volcanic and shallow intrusive rock in Mount Sinabung. Then, inactive faults crosswise over Tinggi Raja came after seismic activity for more than one decade of Sinabung volcanic activity (Mccausland et al., 2019). At well-monitored Sinabung volcanoes, the long-term eruption is forecast for lava and ash cloud column outpouring. The increase in Sinabung's volcanic behavior is of tremendous significance in the paper by Primulyana et al. FMA helped improve the clarity of the information and revealed less correlated volcanic manifestation to geothermal trigger due to inconsistency of the magnetic field anomaly in geothermal resources. It causes the travertine heap will cover the flow of hot water on the surface so that hot water with higher pressure searches for new output channels as if creating new hot springs or the transfer of hot springs on the surface.

On the other hand, one geothermal prospect area in the Simalungun district is founded at 02°36-15 ″-03°18-06″ LU and 98°32′06" - 99°34′28″ BT. From previous research, geomagnetic and geoelectric methods were effective methods to find out the point of the prospect of geothermal energy. The existing geothermal energy development in North Sumatra is found in Sarulla (330 MW), Sibayak (120 MW), and Dolok Marawa Tinggi Raja Simalungun Regency, with a potential

reserve of 38 MW. North Sumatra is one of Indonesia's most geothermal energy potentials, with 1,857.00 MW in six districts, Karo, Simalungun, North Tapanuli, South Tapanuli, Padang Lawas, and Mandailing Natal (National Development Planning Agency (Bappenas), 2020). Geothermal is an alternative energy that can be renewed (renewable). Geothermal power plants are a great solution to solve the lack of energy that has the advantages of geothermal energy, such as being environmentally friendly and including energy that cannot be exported so that the electricity supply in Indonesia continues to be maintained for hundreds of years (Milousi et al., 2022).

6. Conclusions

The field modeling analysis (FMA) is applied to find the influence of the Sinabung eruption and geothermal Tinggi Raja. Low magnetic field anomalies in geothermal resources inverse correlate volcanic manifestation to geothermal trigger. Distance, type, and felt volcanic earthquake and eruption are less direct impact between the blast of Mount Sinabung and the displacement of springs at Tinggi Raja. Furthermore, subsurface information from FMA has limited information because geomagnetic coverage is short. So, FMA indicates the obstruction of the surface in a hot spring due to heating the water fluid high enough continuously, causing clumping of hot water (travertine) in the outlet of the hot water in the fault field. As a result, the travertine heap will cover the flow of hot water on the surface so that hot water with higher pressure searches for new output channels as if creating new hot springs or the transfer of hot springs on the surface.

Author contribution form

Togi Tampubolon: Conceptualization, Methodology/Study design, Validation, Formal analysis, Resources, Writing – original draft, Writing – review and editing, Supervision, Funding acquisition, Jeddah Yanti: Conceptualization, Methodology/Study design, Software, Validation, Formal analysis, Investigation, Resources, Data curation, Writing – original draft, Writing – review and editing, Visualization, Project administration, Rita Juliani: Conceptualization, Methodology/Study design, Validation, Formal analysis, Investigation, Resources, Data curation, Visualization, Supervision, Project administration, Juniar Hutahaean: Conceptualization, Methodology/Study design, Software, Formal analysis, Investigation, Resources, Data curation, Supervision, Project administration.

Declaration of competing interest

The authors declare that they have no known competing financial interests or personal relationships that could have appeared to influence the work reported in this paper.

Data availability

No data was used for the research described in the article.

References

Andreastuti, S., Paripurno, E.T., Gunawan, H., Budianto, A., Syahbana, D., Pallister, J., 2019. Character of community response to volcanic crises at Sinabung and Kelud volcanoes. J. Volcanol. Geoth. Res. 382, 298–310. https://doi.org/10.1016/j.jvolgeores.2017.01.022.

Ashat, A., Pratama, H.B., Itoi, R., 2019. Comparison of resource assessment methods with numerical reservoir model between heat stored and experimental design: case study Ciwidey-Patuha geothermal field. IOP Conf. Ser. Earth Environ. Sci. 254 (1) https://doi.org/10.1088/1755-1315/254/1/012011.

Awaliyatun, F.Z., Hutahaean, J., 2015. Penentuan Struktur Bawah Permukaan Tanah daerah Potensi panas bumi dengan Metode Geomagnetik di Tinggi Raja kabupaten simalungun. Jurnal Einstein 3 (1), 1–8.

Bhakti, H.H., 2011. Magma Genesis in Kabanjahe region Continental Margin arc of Sumatra Genesis magma di Daerah Kabanjahe Busur Tepi Benua Sumatra. Indonesian J. Geosci. 6 (2), 105–127. http://ijog.bgl.esdm.go.id.

BNPB, 2013. Riwayat Letusan Sinabung. In Majalah Gema BNBP 4 (3).

BNPB, 2016. Info bencana BNPB. Info Bencana. Informasi Kebencanaan Bulanan Teraktual 1–4.

Carr, B.B., Clarke, A.B., Vanderkluysen, L., Arrowsmith, J.R., 2019. Mechanisms of lava flow emplacement during an effusive eruption of Sinabung Volcano (Sumatra, Indonesia). J. Volcanol. Geoth. Res. 382, 137–148. https://doi.org/10.1016/j.jvolgeores.2018.03.002. January 2014.

Center for Volcanology and Geological Hazard Mitigation. 2020. Life series volcano observatory Notice for Aviation. Geological Agency of the Indonesian Ministry of Energy and Mineral Resources, Indonesia. https://magma.esdm.go.id/v1/vona?code=SIN.

Ekinci, Y.L., Balkaya, Ç., Şeren, A., Kaya, M.A., Lightfoot, C.S., 2014. Geomagnetic and geoelectrical prospection for buried archaeological remains on the Upper City of Amorium, a Byzantine city in midwestern Turkey. J. Geophys. Eng. 11 (1) https://doi.org/10.1088/1742-2132/11/1/015012.

Eskandari, A., De Rosa, R., Amini, S., 2015. Remote sensing of Damavand volcano (Iran) using Landsat imagery: implications for the volcano dynamics. J. Volcanol. Geoth. Res. 306, 41–57. https://doi.org/10.1016/J.JVOLGEORES.2015.10.001.

Gunawan, H., Surono Budianto, A., Kristianto Prambada, O., McCausland, W., Pallister, J., Iguchi, M., 2019. Overview of the eruptions of Sinabung Volcano, 2010 and 2013–present and details of the 2013 phreatomagmatic phase. J. Volcanol. Geoth. Res. 382, 103–119. https://doi.org/10.1016/j.jvolgeores.2017.08.005.

Hotta, K., Iguchi, M., Ohkura, T., Hendrasto, M., Gunawan, H., Rosadi, U., Kriswati, E., 2019. Magma intrusion and effusion at Sinabung volcano, Indonesia, from 2013 to 2016, as revealed by continuous GPS observation. J. Volcanol. Geoth. Res. 382, 173–183. https://doi.org/10.1016/j.jvolgeores.2017.12.015.

Indrastuti, N., Nugraha, A.D., McCausland, W.A., Hendrasto, M., Gunawan, H., Kusnandar, R., Kasbani, Kristianto, 2019. 3-D seismic tomographic study of Sinabung volcano, northern Sumatra, Indonesia, during the inter-eruptive period October 2010–July 2013. J. Volcanol. Geoth. Res. 382, 197–209. https://doi.org/10.1016/j.jvolgeores.2019.03.001.

Kab Simalungun, B.P.S., 2021. Simalungun Dalam Angka 2021, 357.

Kabupaten Karo, B.P.S., 2021. Kabupaten Karo dalam Angka 2021. Kabanjahe: BPS 320.

Karolina, R., Syahrizal, Putra M.A., Prasetyo, T.A., 2015. Optimization of the use of volcanic ash of Mount Sinabung eruption as the substitution for fine aggregate. Procedia Eng. 125, 669–674. https://doi.org/10.1016/j.proeng.2015.11.102.

Kriswati, E., Meilano, I., Iguchi, M., Abidin, H.Z., Surono, 2019. An evaluation of the possibility of tectonic triggering of the Sinabung eruption. J. Volcanol. Geoth. Res. 382, 224–232. https://doi.org/10.1016/j.jvolgeores.2018.04.031.

Li, Z., Fu, G., 2019. Application of magnetic susceptibility parameters in research of Igneous rock in Chepaizi. J. Phys. Conf. 1176 (4) https://doi.org/10.1088/1742-6596/1176/4/042068.

Marwan, M., Yanis, M., Nugraha, G.S., Zainal, M., Arahman, N., Idroes, R., Dharma, D.B., Saputra, D., Gunawan, P., 2021. Mapping of fault and hydrothermal system beneath the seulawah volcano inferred from a magnetotellurics structure. Energies 14 (19), 1–22. https://doi.org/10.3390/en14196091.

Mccausland, W.A., Gunawan, H., White, R.A., Indrastuti, N., Patria, C., Suparman, Y., Putra, A., Triastuty, H., Hendrasto, M., 2019. Using a process-based model of pre-eruptive seismic patterns to forecast evolving eruptive styles at Sinabung Volcano, Indonesia. J. Volcanol. Geoth. Res. 382, 253–266. https://doi.org/10.1016/j.jvolgeores.2017.04.004.

Milousi, M., Pappas, A., Vouros, A.P., Mihalakakou, G., Souliotis, M., Papaefthimiou, S., 2022. Evaluating the Technical and Environmental Capabilities of Geothermal Systems through Life Cycle Assessment.

Mohamed El-Desoky, H., Soliman, N., Ahmed Heikal, M., Moustafa Abdel-Rahman, A., 2021. Mapping hydrothermal alteration zones using ASTER images in the Arabian–Nubian shield: a case study of the northwestern Allaqi district, South Eastern Desert, Egypt. J. Asian Earth Sci. X (5) https://doi.org/10.1016/j.jaesx.2021.100060.

Nakada, S., Zaennudin, A., Yoshimoto, M., Maeno, F., Suzuki, Y., Hokanishi, N., Sasaki, H., Iguchi, M., Ohkura, T., Gunawan, H., Triastuty, H., 2019. Growth process of the lava dome/flow complex at Sinabung Volcano during 2013–2016. J. Volcanol. Geoth. Res. 382, 120–136. https://doi.org/10.1016/j.jvolgeores.2017.06.012.

National Development Planning Agency (Bappenas), 2020. Presidential decree No. 18 Year 2020. National Mid-Term Development Plan 2020–2024, 313. https://www.bappenas.go.id/id/data-dan...dan.../rpjmn-2015-2019/.

Neale, C.M.U., Jaworowski, C., Heasler, H., Sivarajan, S., Masih, A., 2016. Hydrothermal monitoring in Yellowstone National Park using airborne thermal infrared remote sensing. Rem. Sens. Environ. 184, 628–644. https://doi.org/10.1016/j.rse.2016.04.016.

Nugraha, A.D., Indrastuti, N., Kusnandar, R., Gunawan, H., McCausland, W., Aulia, A.N., Harlianti, U., 2019. Joint 3-D tomographic imaging of Vp, Vs and Vp/Vs and hypocenter relocation at Sinabung Volcano, Indonesia from November to December 2013. J. Volcanol. Geoth. Res. 382, 210–223. https://doi.org/10.1016/j.jvolgeores.2017.09.018.

Nukman, M., Hochstein, M.P., 2019. The Sipoholon Geothermal Field and adjacent geothermal systems along the North-Central Sumatra Fault Belt, Indonesia: reviews on geochemistry, tectonics, and natural heat loss. J. Asian Earth Sci. 170, 316–328. https://doi.org/10.1016/j.jseaes.2018.11.007. February 2018.

Octavani, A.S., Kadri, M., 2019. Analisis Resistivitas Bawah Permukaan Menggunakan Metode Geolistrik Konfigurasi Wenner–Schlumberger dan Dipole-Dipole di daerah geothermal Gunung Sibayak kabupaten Karo Provinsi sumatera utara. EINSTEIN E-JOURNAL 6 (2). https://doi.org/10.24114/einstein.v6i2.12075.

Pallister, J., Wessels, R., Griswold, J., McCausland, W., Kartadinata, N., Gunawan, H., Budianto, A., Primulyana, S., 2019. Monitoring, forecasting collapse events, and mapping pyroclastic deposits at Sinabung volcano with satellite imagery.

J. Volcanol. Geoth. Res. 382, 149–163. https://doi.org/10.1016/j.jvolgeores.2018.05.012.

Primulyana, S., Kern, C., Lerner, A.H., Saing, U.B., Kunrat, S.L., Alfianti, H., Marlia, M., 2019. Gas and ash emissions associated with the 2010–present activity of Sinabung Volcano, Indonesia. J. Volcanol. Geoth. Res. 382, 184–196. https://doi.org/10.1016/j.jvolgeores.2017.11.018.

Reda, T.M., Gebrehiwot, W.Z., Jothimani, J.M., Tirusew, S.Y., 2022. Assessing the effect of volcano-tectonic activity on the spatial distribution of surface temperature in the Main Ethiopian Rift, using integrated approach of remote sensing data. Eur. J. Rem. Sens. 55 (1), 86–102. https://doi.org/10.1080/22797254.2021.2021555.

Sharma, P., 2012. Magnetic surveying. Environ. Eng. Geosci. 65–111. https://doi.org/10.1017/cbo9781139171168.004.

Sullivan, G.B., Sagala, S., 2020. Quality of life and subjective social status after five years of Mount Sinabung eruptions: disaster management and current sources of inequality in displaced, remaining and relocated communities. October 2019 Int. J. Disaster Risk Reduc. 49, 101629. https://doi.org/10.1016/j.ijdrr.2020.101629.

Sundhoro, H., BakrunSuryakusuma, D., Sulaeman, B., Situmorang, T., 2006. Survei panas bumi terpadu (geologi, geokimia dan geofisika) daerah dolok marawa, kabupaten simalungun - sumatera utara. Pemaparan Hasil Kegiatan Lapangan Subdit Panas Bumi.

Yan, Y., Zhou, X., Liao, L., Tian, J., Li, Y., Shi, Z., Liu, F., Ouyang, S., 2022. Hydrogeochemical characteristic of geothermal water and precursory anomalies along the Xianshuihe fault zone, southwestern China. Water (Switzerland) 14 (4). https://doi.org/10.3390/w14040550.